Progress In Electromagnetics Research M, Vol. 47, 77–86, 2016

The Cherenkov Emission in Regular and Random Photonic Crystals

Gennadiy Burlak* **and Erika Martínez-Sánchez**

Abstract—We systematically study the Cherenkov optical emission by a nonrelativistic charge uniformly moving in parallel to surface of a photonic crystal by FDTD simulations. It is found that a near-static structure of field oscillations produced by a discontinuity of dielectric permittivity in surface of photonic lattice is generated. Such oscillations have large amplitude in Cherenkov group cone and generate a number of well defined spectral resonances corresponding to eigenmodes of the photonic grid. The dynamics and field properties in photonic lattice with random vacancies are investigated too. It is found that even at medium level of a random perturbation the field shape shows the structural stability of the Cherenkov emission field in a photonic crystal.

1. INTRODUCTION

Photonic nanostructures, which can manipulate the light waves or photons in all dimensions, represent a significant rise to the next-generation nanophotonic technology [1]. Such nanostructures allow perfect integration with currently using optical-electronic materials and devices with various extension of the Cherenkov effect [1–21]. Recently extensive efforts have been devoted to fabricating the photonic nanostructures with controlled symmetry, size and defects on a large scale [1–5]. A very recent experiment [21] registers soliton induced Cherenkov radiation that allows coherence over a spectral bandwidth (phase-stabilize to the sub-Hertz level) in a photonic chip.

The Cherenkov emission occurs when a charged particle propagates inside a dielectric medium with a velocity larger than the electromagnetic wave phase velocity of the medium [6]. A particle with velocity exceeding such a threshold gives rise to a conical wave front (see, e.g., [7, 8]).

In the case of a long photonic crystal (long-range periodicity) one can use periodic boundary conditions. The latter allows decomposition of electromagnetic waves to series of Bloch waves that finally generate the frequencies spectrum with allowed bandgap structure [1]. The study of Cherenkov emission for such a situation can be done by the use of standard technique [2]. However, if a photonic crystal is not long (such that the long-range symmetry is broken), the periodic boundary conditions cannot be applied. In this case, the electromagnetic waves (generated by the Cherenkov emission) are not longer than the exact Bloch waves because the group velocity is not given by the dispersion of the frequency the Bloch wavevectors. Furthermore, in the photonic crystals with randomly valued depth of holes, even a short-range order becomes not valid. The question then arises about the structural stability of the optical modes in photonic crystals with randomness of lattice. Nowadays such systems are of considerable practical interest. Moreover, in such disorder environments it is possible to observe the fundamental optical phenomena as the optical Anderson localization [22]. Such a setup in disordered environments may lead to lasing (random laser) [23, 24].

For this situation, the use of numerical methods (FDTD) [9, 26] is highly desired to explore the dynamics of optical waves (associated with the Cherenkov emission) in the photonic crystal. However,

Received 17 December 2015, Accepted 19 March 2016, Scheduled 27 March 2016

* Corresponding author: Gennadiy Burlak (gburlak@uaem.mx).

The authors are with the Centro de Investigación en Ingeniería y Ciencias Aplicadas, Universidad Autónoma del Estado de Morelos, Cuernavaca, Mor., México.

such a 3D problem is too complicated for an analytical consideration. The numeric FDTD simulation of field spatial dynamics with the use of absorbing boundary conditions in a photonic lattice $(x; y)$ has to be applied.

In this paper, we study the Cherenkov optical emission by a nonrelativistic charge uniformly moving in parallel to surface of a photonic crystal (PCr). To do that, we perform FDTD simulations in 3D perforated slab and study a dynamics of near-static field produced by the discontinuity of dielectric permittivity in the photonic structure. We use the fact that some fraction of the incident radiation is transmitted through the discontinuity of the dielectric permittivity of PCr lattice and generates a near-field interference pattern of the transmitted light. Such an interference picture gives important information on the field phase distribution. We have found that such dynamics produces a number of well-defined spectral peaks in the frequency domain. The dynamics for a disordered PCr, where the holes in slab deviate randomly (lattice vacancy), is studied too. In the latter case, the short-range order is not valid, so the particular holes can affect the total properties of optical modes in the photonic crystal.

2. BASIC EQUATIONS

The Maxwell equations read $\nabla \times \mathbf{E} = -\mu_0 \frac{\partial \mathbf{H}}{\partial t}$, $\nabla \times \mathbf{H} = \varepsilon_0 \varepsilon \frac{\partial \mathbf{E}}{\partial t} + q\mathbf{v}_0 f(r,t)$, where $\varepsilon = \varepsilon(\mathbf{r})$ is a dielectric permittivity of the dielectric PCr structure [7]. We consider the charge particle (charge q) moving with a uniform velocity $\mathbf{v}_0$ closely to $(x, y$ surface) parallel to y direction: $\mathbf{v}_0 \parallel \widehat{\mathbf{e}}_y$ and the density of particles (bunch) is defined by the Gaussian as $f(r,t) = W^{-3} \exp\{-[x^2 + (y - v_0 t)^2 + z^2]/W^2\}$, where W is the width; at $W \to 0$ such a distribution is simplified to the isotropic point-source distribution $f(r,t) \to (\pi)^{3/2} \delta(x)\delta(y - v_0 t)\delta(z)$. In the following simulations, we use dimensionless variables, where for renormalization are used: the vacuum light velocity $c = (\varepsilon_0 \mu_0)^{-0.5}$ and the typical spatial scale for nanooptics objects $l_0 = 500nm$. The electric and magnetic fields are renormalized with the electrical scale $E_0 = q l_0 \varepsilon_0$ and magnetic scale $H_0 = (\varepsilon_0/\mu_0)^{0.5} E_0$, respectively.

3. NUMERICS

3.1. Regular Lattice

A typical structure of the considered PCr is shown in Figure 1.

Figure 1. A free no-magnetic slab with dielectric permittivity ε_S is assumed as a platform for PCr perforated lattice.

A free-standing (no magnetic) PCr slab structure is assumed as a platform for a PCr lattice. We perform FDTD simulations to study a structure of field in such the photonic system. The normalized numerical velocity of the propagating field in 3D homogeneous numerical grid is $dl/dt = \sqrt{3} dx/dt$ (with $dx = dy = dz$) [9]. In what follows, we use renormalized variables $dx/dt \to 3dx/dt = (\sqrt{3}) dl/dt = c_n \equiv$

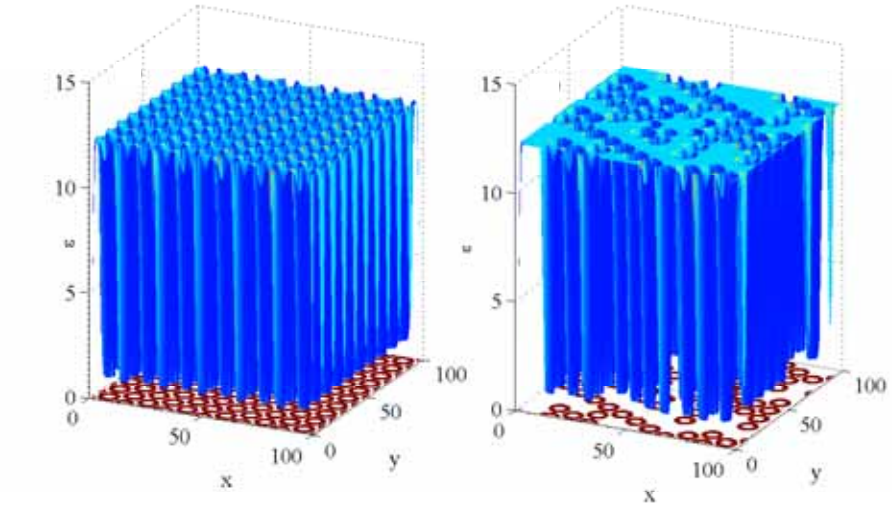

Figure 2. (Color on line) The average dielectric permittivity of a photonic crystal $\varepsilon(x, y)$ where the dielectric slab ($\varepsilon_S = 12.25$) is perforated by holes ($\varepsilon_h = 1$) with (a) regular lattice, and (b) random lattice with control parameter $p = 0.5$, see more details in Section 3.2.

1.732 that is the "*vacuum light velocity*" in the numerical grid, such that $c_n > v_0$. Another important velocity is $c_{cr} = c_n/|n|$ corresponding to the critical velocity of bunch v_0 when the Cherenkov radiation appears in a dispersiveless dielectric with refraction index n, and the time step is $dt = 0.00088$. In our study, we use the approach [12] which we have extended and adopted for our purposes.

Figure 2 displays the average dielectric permittivity of a photonic crystal $\varepsilon(x, y)$ for (a) regular lattice and (b) random lattice.

An important property of the considered PCr is that the standard boundary conditions for the normal components of the electric displacement D_n [7] in the holes wells $\varepsilon_h E_{hn} = \varepsilon_S E_{Sn}$ (here E_{hn}, E_{Sn} are normal components of the electric fields in the boundary hole and slab respectively) produce discontinuity of the normal $E_{x,y}$ field components, which leads to discontinuity of local field generated by moving particle in area of periodic holes.

We apply the FDTD technique to study the emission field dynamics in such an advanced medium. Our results are shown in Figures 3–10. In our FDTD simulation, we used a sufficiently large horizontal computational domain $L^2 = (16l_0 \times 16l_0)$, where $l_0 = 500\,\text{nm}$ and $\mp L/2$ indicate the input and output points, respectively. The optical loss of the resonant mode is closely related to the in-plane field distributions.

First for reference purposes we simulate the Cherenkov radiations in a dispersiveless dielectric for homogeneous case $\varepsilon_S = \varepsilon_h = 1.44$ for $c_n > v_0 = 1.5 > c_{cr} = 1.2$ at the time when the particle touches the output boundary. In Figure 3(a), we observe the standard Cherenkov wave cone with the angle of emission θ_c relative to the velocity of particle as $\cos(\theta_c) = c/nv_0$, see Chap. 13 in [7], Chap. 2 in [8].

More interesting is the case when the dielectric permittivity of the slab and holes have distinct values $\varepsilon_S \neq \varepsilon_h$. Figure 3 displays snapshots of field $E_x(x, y)$ distribution in plane (x, y) for particle moving with overcritical velocity $v_0 = 1.5$ and different 2D photonic crystals with slab perforated by holes: (a) homogeneous case $\varepsilon_S = \varepsilon_h = 1.44$; (b) $\varepsilon_S = 1.44$, $\varepsilon_h = 1$; (c) $\varepsilon_S = 5$, $\varepsilon_h = 1$; (d) $\varepsilon_S = 12.25$, $\varepsilon_h = 1$. From Figures 3(b)–(d) cases one can see significantly inhomogeneous field oscillations within the Cherenkov cone. Since the spatial period of PCr is comparable with the field wavelength $l_0/\lambda \leq 1$ such a 2D system acts as a distributed 2D plane resonator having a special eigenfrequency spectrum.

In this case, we deal with highly dispersive media where the field intensity is peaked on the surface of a group cone (see [25] and references therein) that is neither orthogonal to the phase nor to the group velocity of the emitted light and is much narrower than the Cherenkov wave cone.

From Figures 3(b)–(d) we observe that for such a geometry the field within the Cherenkov cone acquires highly inhomogeneous structure relating the structure of holes in PCr due to the discontinuity

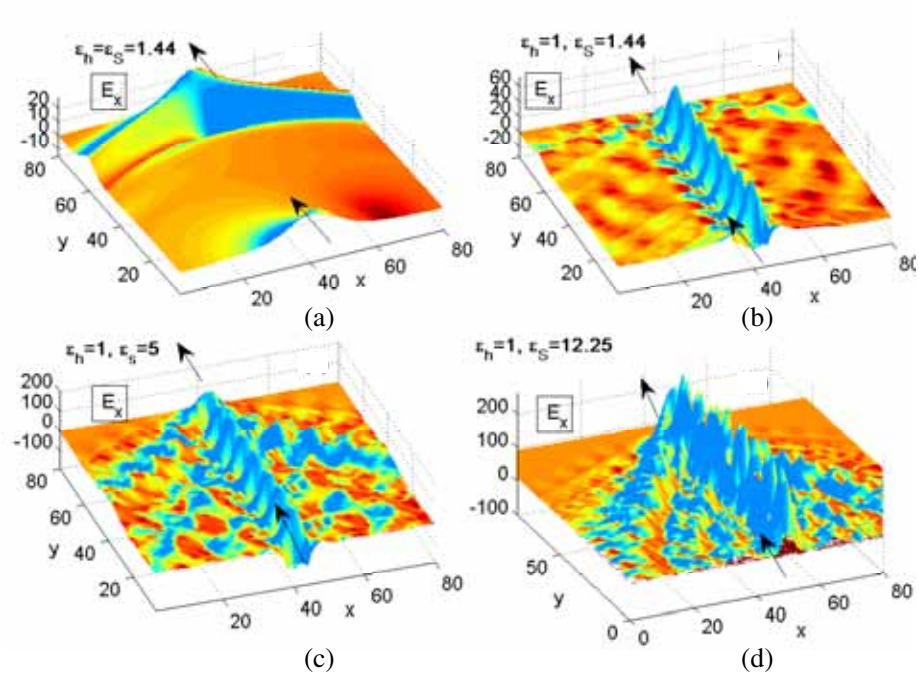

Figure 3. (Color on line) Snapshots the field $E_x(x, y)$ in plane (x, y) for particle moving with overcritical velocity $v_0 = 1.5$ and different ε_S of 2D photonic crystals slab perforated by holes $\varepsilon_h = 1$, (a) homogeneous case $\varepsilon_S = \varepsilon_h = 1.44$; (b) $\varepsilon_S = 1.44$, $\varepsilon_h = 1$; (c) $\varepsilon_S = 5$, $\varepsilon_h = 1$; (d) $\varepsilon_S = 12.25$, $\varepsilon_h = 1$. Incoming arrows show the enter points of the particle.

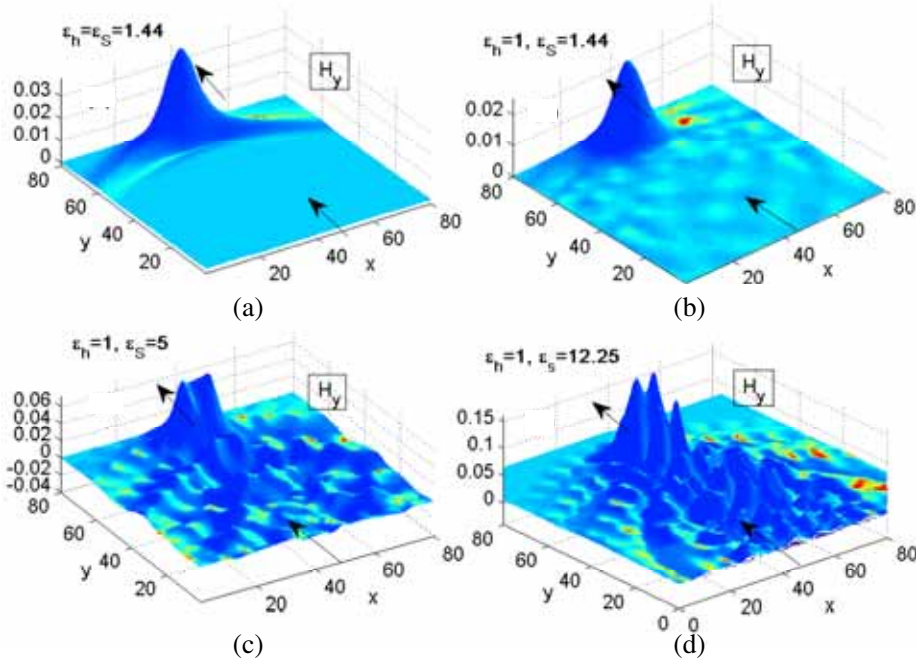

Figure 4. (Color on line) The same as in Figure 3 but for magnetic component $H_y(x, y)$, (a) homogeneous case $\varepsilon_S = \varepsilon_h = 1.44$; (b) $\varepsilon_S = 1.44$, $\varepsilon_h = 1$; (c) $\varepsilon_S = 5$, $\varepsilon_h = 1$; (d) $\varepsilon_S = 12.25$, $\varepsilon_h = 1$. Incoming arrows show the enter points of the particle.

of the dielectric permittivity $\varepsilon(x, y)$. Moreover, Figures 3(b)–(d) show that the amplitude of the field oscillations $E_x(x, y)$ have maximal values in the narrow group cone [25] closely to the path of the charged particle. In the considered case $\varepsilon_h < \varepsilon_S$ so the field is localized in the holes area and exponentially decays beyond the holes [7]. For such a reason, the amplitudes of near-static oscillations decay slowly even after the particle has leaved the system (for $t > L/v_0$).

A simple physical interpretation of the group cone can be put forward in terms of group velocity considering that for each direction around the charge velocity, the burst of Cherenkov light is emitted into a group of modes while the peak of the pulse moves in space with a velocity equal to the group velocity $\mathbf{v}_g$ experiencing an almost negligible absorption [25].

Figure 4 displays the magnetic field $H_y(x, y)$ for the parameters used in Figure 3, respectively.

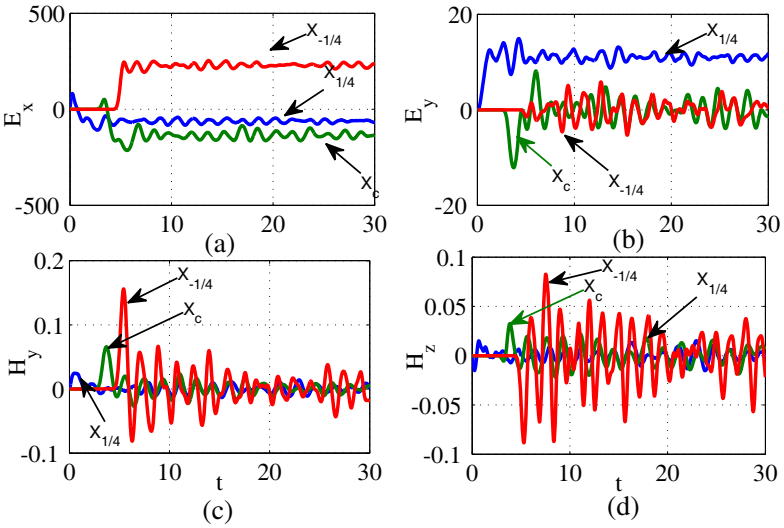

Figure 5. (Color on line) The time dependence of electric and magnetic field components in various points along the charge path at $X_{\pm 1/4}, X_c$ at $x = \pm L/4, 0$ for field shown in Figures 3(d): (a) $E_x(t)$, (b) $E_y(t)$, (c) $H_y(t)$, (d) $H_z(t)$.

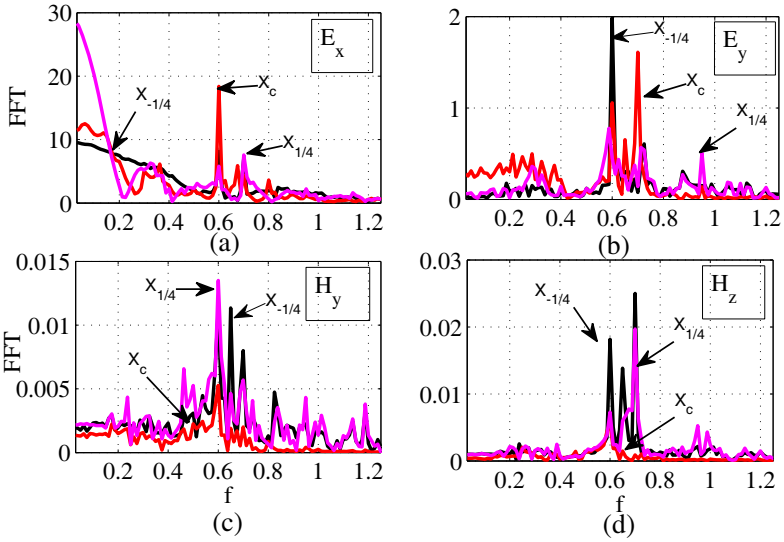

Figure 6. (Color on line) The frequency (FFT) spectrum of electromagnetic oscillations shown in Figure 5 for various points along the charge path at $X_{\pm 1/4}, X_c$ at $x = \pm L/4, 0$ having highest spectral peaks. Such oscillations correspond to optical eigenmodes of PCr excited by the moving charged particle: (a) $E_x(f)$, (b) $E_y(f)$, (c) $H_y(f)$, (d) $H_z(f)$. Here and in follows y-axis exhibits the amplitude of FFT.

Since we consider the no-magnetic PC slab, there is no magnetic inhomogeneity in the system. The magnetic field is defined from equation $\frac{\partial \mathbf{H}}{\partial \mathbf{t}} = -(\mathbf{1}/\mu_\mathbf{0})\nabla \times \mathbf{E}$, and thus it is small (see Figure 4).

It is instructive to study the field dynamics (associated with the Cherenkov emission) along the path of the moving particle. To do that we explore the time dependence of E_x in various points along the charge path (group cone), shown in Figure 3(d).

Figure 5 shows the time dependence of field at a long-time ($t > L/v_0$) simulation. From Figures 5(c), (d) we observe that the expected field $H_{y,z}(x, y)$ has smoother shape with a regular spatial structure.

From Figure 5(a) we observe that $E_{x,y}$ amplitudes have oscillating shape shifted with a pedestal defined by a point position. Figures 5(c), (d) show that $H_{y,z}$ oscillates in vicinity of zero, which is natural due to the continuity of magnetic field in the system. It is interesting to study from Figure 5 which of such oscillations correspond to eigenmode in a gap zone of PCr. Such a spectrum is shown in Figure 6 for some highest spectral peaks corresponding to long-live modes in PCr. We notice the existence of near-static, nonradiating field artificial peak around $f = 0$ in Figure 6(a) (see discussion in [2]). The value of such a resonance can be evaluated from a simple dimension relation $f = c/\lambda\sqrt{\varepsilon_p}$, where ε_p is a weighted dielectric permittivity of PCr $\varepsilon_p = (\varepsilon_S(V_S - V_c) - \varepsilon_h V_c)/(V_S + V_c)$ and V_S the volume of slab reduced by the volume of all holes V_c. In our dimensionless case $Vc = 338\pi R^2 h = 65.0$, $V_S = 432$, $\lambda = 1$, $c = 1.732$, $h = 0.5$, $\varepsilon_h = 1$ that gives $f_0 = 0.58$ and corresponds to resonances in a range $f_0 \sim 0.6$ shown in Figure 6.

3.2. Photonic Crystal with Random Vacancies in a Lattice

In real situation, the depth of holes (or high of cylinders in the contrast configuration) can have a random deviation. The latter leads to spatial variations of the average dielectric permittivity that acquires the randomly perturbed structure. In what follows we consider a photonic random system where in the reference lattice the nodes can have a lattice vacancy that allows being zero of the depths of some holes. The average dielectric permittivity of such a system is displayed in Figure 2, panel (b). We represent such a system by a number of vacancies N_v with a control parameter $p = N_v/N_0$, where N_0 is the total number of holes. In a periodic photonic crystal $N_v = 0$, so $p = 0$.

We simulate the random vacancies as following. We characterize the photonic structure by random factor m_γ so that $m_\gamma = 0$ ($\gamma < p$), and $m_\gamma = 1$ ($\gamma \geq p$), where γ is the uniform distributed random

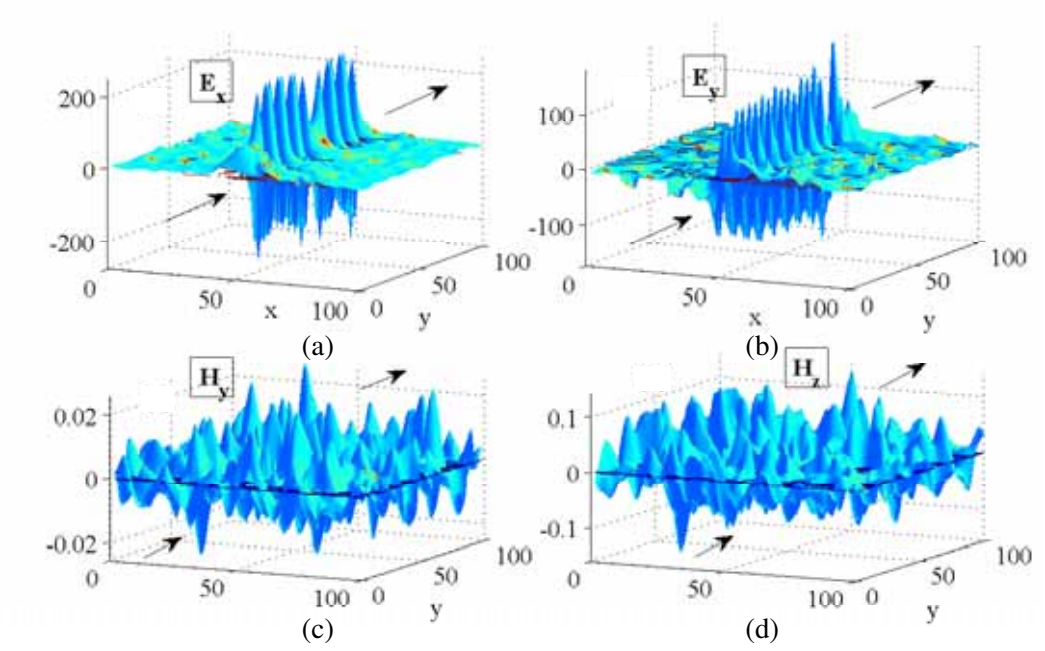

Figure 7. (Color on line) The spatial (x, y) shape of field components: (a) $E_x(x, y)$, (b) $E_y(x, y)$, (c) $H_y(x, y)$, (d) $H_z(x, y)$ for a random PCr with $p = 0.5$.

numbers in $[0, 1)$ and p the control parameter that characterize the level of randomness in the lattice. (In first part of the paper it is considered the regular lattice with $p = 0$ that gives $m_\gamma = 1$.) We define the actual depth $h_{i,j}$ of a lattice hole in node (i, j) as $h_{i,j} = m_\gamma h$ (for fixed p), where h is a reference hole depth. This allows simulating the random PCr for the case when some of the holes are vacant (or have zero depths). Corresponding dielectric permittivity $\varepsilon = \varepsilon(x, y)$ is displayed in Figure 2, panel (b) for $p = 0.5$.

We calculate the spectrum of electromagnetic field oscillations for various levels of randomness defined by control parameter p. Figure 7 shows the spatial structure of the field at a randomly prepared structure with control parameter $p = 0.5$ at long-time simulation for $t \cong L/v_0$. From Figure 7(a) we observe that already for a medium random perturbation level with $p = 0.5$ the electric field $E_x(x, y)$ has rather similar shape to that in Figures 3(c), (d). The amplitudes of magnetic field in Figures 7(c), (d) remain small and have an irregular structure. From the comparison between Figure 3 and Figure 7, we observe a close similarity of the field radiated by charged particle in PCr for periodic and randomly perturbed field shapes even for medium perturbation level $p = 0.5$. This again exhibits the structural stability of the longitude field E_x distribution in PCr due to discontinuity of field in the boundary of holes.

Figure 8 shows such a spectrum for E_z in the group cone along the charge path at $X_{-1/4}, X_c$ at $x = \pm L/4, 0$ and random PCr for (a) $p = 0$; (b) $p = 0.2$; (c) $p = 0.5$; (d) $p = 0.62$. From Figure 8(a), we observe that the resonance at $f = 0.59$ splits in narrower peaks at the increase of parameter p. However, the resonant zone is concentrated closely to $f \sim 0.6$. This again indicates the structural stability of field modes associated with Cherenkov emission.

It is instructive to study the time dependencies of field's amplitudes for the random and periodic PCr cases in the path of particle. Figure 9 shows such dependencies for PCr with $p = 0.5$ in points close to $x = 0$. From Figure 10 one can see the spectral peak for component E_y at point $x = 0$ near $f = 0.6$ in such random PCr with $p = 0.5$. Similar spectral resonance is also observed for field component E_z in Figure 8. Thus our numerical calculations indicate the structural stability of the resonances at the

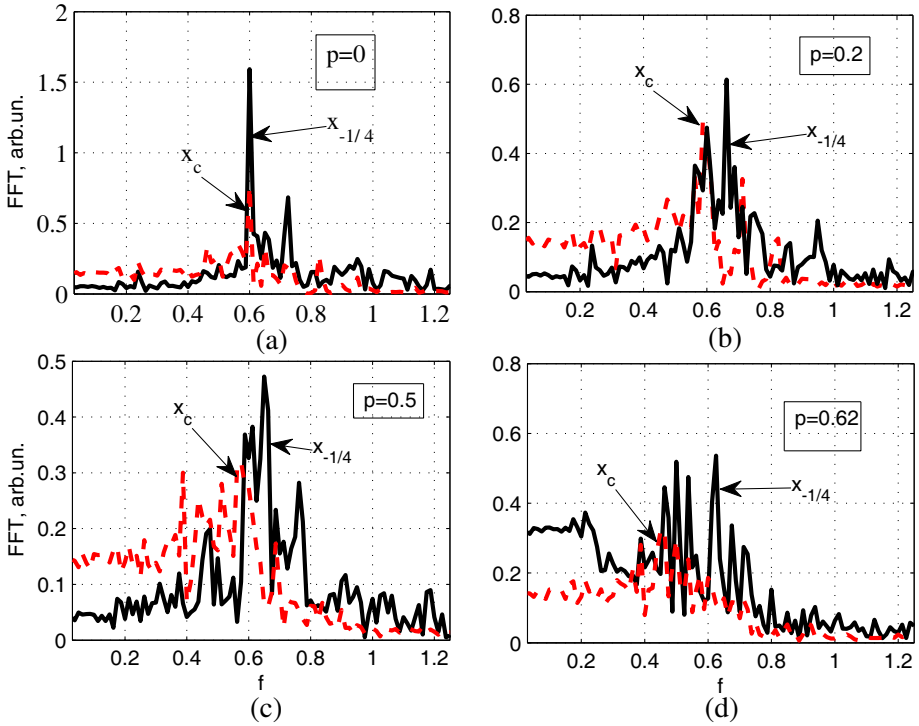

Figure 8. (Color on line) The spectrum of highest resonances of field oscillations E_z in the group cone at $X_{-1/4}, X_c$ at $x = -L/4, 0$ and random PCr and various values parameter p: (a) $p = 0$; (b) $p = 0.2$; (c) $p = 0.5$; (d) $p = 0.62$.

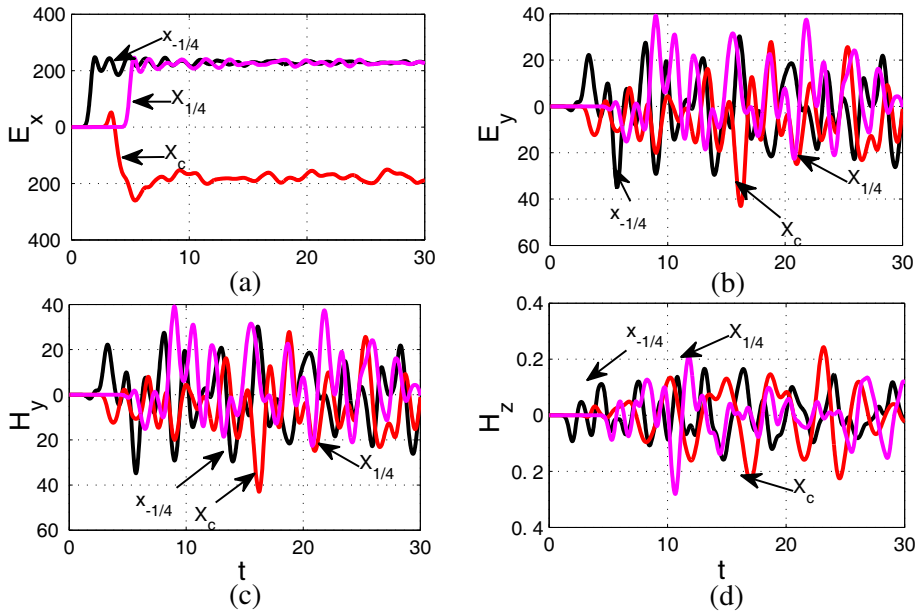

Figure 9. (Color on line) The time dependence of electromagnetic fields in various points in the group cone along the charge path at $X_{\pm 1/4}, X_c$ at $x = \pm L/4, 0$ respectively for random PCr with control parameter $p = 0.5$: (a) $E_x(t)$, (b) $E_y(t)$, (c) $H_y(t)$, (d) $H_z(t)$.

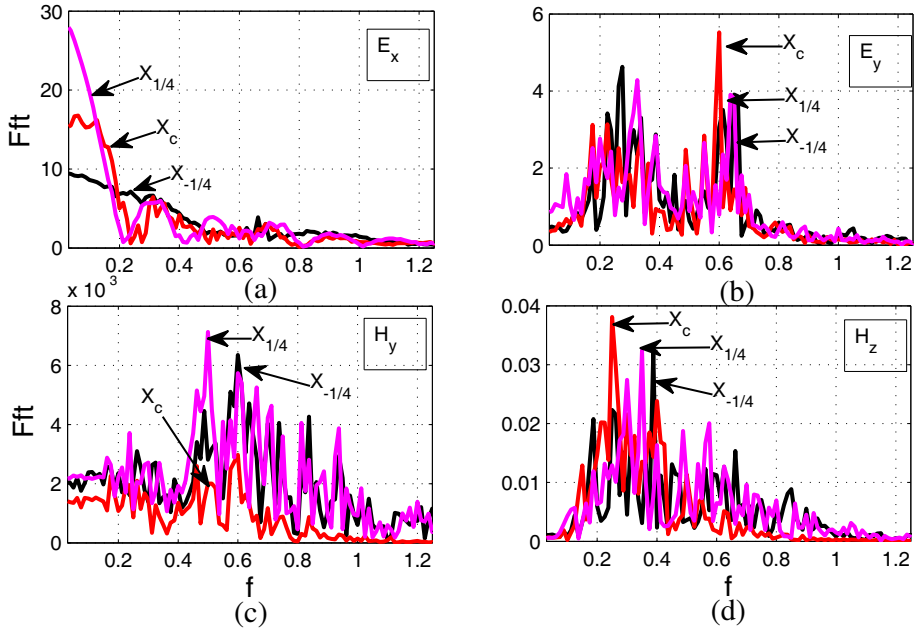

Figure 10. (Color on line) The frequency (FFT) spectrum of electromagnetic oscillations for various points along the charge path. It is shown the oscillations in position at $X_{\pm 1/4}, X_c$ at $x = \pm L/4, 0$ having highest spectral peaks. Such oscillations correspond to optical eigenmodes of PCr excited by the moving charged particle for random PCr with $p = 0.5$, (a) $E_x(f)$, (b) $E_y(f)$, (c) $H_y(f)$, (d) $H_z(f)$.

change of the randomness level photonic crystals. Such resonances respond to generation of a remanent near-static field oscillations in photonic crystals by the charged particle. Due to structural stability such an effect can find applications in modern nanotechnology. As far as in a photonic crystal it is possible to create characteristic radiation patterns without a particle velocity threshold.

4. CONCLUSION

We study Cherenkov optical emission by a nonrelativistic charge uniformly moving parallel to surface of a 2D photonic crystal. It is found that a near-static structure of field oscillations produced by a contrast of dielectric permittivity in the surface of photonic lattice is generated. Such oscillations have large amplitude in the Cherenkov group cone and produce a number of well defined spectral resonances corresponding to eigenmodes of the photonic grid. The dynamics and field properties of a randomly perturbed photonic lattice indicate that even at medium level of a randomness, the field shape has structural stability of the Cherenkov emission in a photonic crystal.

ACKNOWLEDGMENT

The work is partially supported by CONACyT (México) grants No. 169496 and No. 168104.

REFERENCES

1. Joannopoulos, J. D., S. G. Johnson, J. N. Winn, and R. D. Meade, *Photonic Crystals Molding the Flow of Light*, Princeton University Press, 2008.
2. Luo, C., M. Ibanescu, S. G. Johnson, and J. D. Joannopoulos, "Cerenkov radiation in photonic crystals," *Science*, Vol. 299, 368–371, 2003.
3. Chang, G., L.-J. Chen, and F. X. Kurtner, "Highly efficient Cherenkov radiation in photonic crystal fibers for broadband visible wavelength generation," *Optics Letters*, Vol. 35, No. 14, 2361–2363, 2010.
4. Shen, X.-W., Y. J.-H. Yuan, KX.-Z. Sang, C.-X. Yu, R. Lan, X. Min, H. Ying, C.-M. Xia, and L.-T. Hou, "Highly efficient Cherenkov radiation generation in the irregular point of hollow-core photonic crystal fiber," *Chinese Phys. B*, Vol. 21, 114102, 2012.
5. Genevet P., D. Wintz, A. Ambrosio, A. She, R. Blanchard, and F. Capasso, "Controlled steering of Cherenkov surface plasmon wakes with a one-dimensional metamaterial," *Nature Nanotechnology*, Vol. 10, 804–809, 2015.
6. Cherenkov, P. A., "Visible emission of clean liquids by action of γ-radiation," *Dokl. Akad. Nauk.*, Vol. 2, 451–454, 1934.
7. Jackson, J. D., *Classical Electrodynamics*, John Willey and Sons, 1998.
8. Afanasiev, G. N., *Cherenkov Radiation in a Dispersive Medium, Vavilov-Cherenkov and Synchrotron Radiation, Fundamental Theories of Physics*, Kluwer Academic Publishers, 2004.
9. Taflove, A. and S. C. Hagness, *Computational Electrodynamics: The Finite-Difference Time-Domain Method*, Artech House, Boston, 2005.
10. Burlak, G., "Spectrum of Cherenkov radiation in dispersive metamaterials with negative refraction index," *Progress In Electromagnetics Research*, Vol. 132, 149–158, 2012.
11. Burlak, G. and E. Martínez-Sánchez, "Change of structure of the Cherenkov emission at modulated source in dispersive metamaterials," *Progress In Electromagnetics Research*, Vol. 139, 277–288, 2013.
12. Kim, S. H., S. K. Kim, and Y. H. Lee, "Vertical beaming of wavelength-scale photonic crystal resonators," *Phys. Rev. B*, Vol. 73, 235117, 2006.
13. Averkov, Yu. O. and V. M. Yakovenko, "Cherenkov radiation by an electron particle that moves in a vacuum above a left-handed material," *Phys. Rev. B*, Vol. 79, 193402–193412, 2005.
14. Xi, S., H. Chen, T. Jiang, L. Ran, J. Huangfu, B. L. Wu, J. A. Kong, and M. Chen, "Experimental verification of reversed cherenkov radiation in left-handed metamaterial," *Phys. Rev. Lett.*, Vol. 103, 194801, 2009.
15. Averkov, Yu. O., A. V. Kats, and V. M. Yakovenko, "Electron beam excitation of left-handed surface electromagnetic waves at artificial interfaces," *Phys. Rev. B*, Vol. 72, 205110–205114, 2005.
16. Zhou, J., Z. Duan, Y. Zhang, M. Hu, W. Liu, P. Zhang, and S. Liu, "Numerical investigation of Cherenkov radiations emitted by an electron beam particle in isotropic double-negative

metamaterials," *Nuclear Instruments and Methods in Physics Research Section A*, Vol. 654, No. 1, 475–480, 2011.

17. Duan, Z. Y., Y. S. Wang, X. T. Mao, W. X. Wang, and M. Chen, "Experimental demonstration of double-negative metamaterials partially filled in a circular waveguide," *Progress In Electromagnetics Research*, Vol. 121, 215–224, 2011.
18. Zhu, L., F.-Y. Meng, F. Zhang, J. Fu, Q. Wu, X. M. Ding, and J. L.-W. Li, "An ultra-low loss split ring resonator by suppressing the electric dipole moment approach," *Progress In Electromagnetics Research*, Vol. 137, 239-254, 2013.
19. Duan, Z., C. Guo, and M. Chen, "Enhanced reversed Cherenkov radiation in a waveguide with double-negative metamaterials," *Opt. Express*, Vol. 19, 13825–13830, 2011.
20. García de Abajo, F. J., A. G. Pattantyus-Abraham, N. Zabala, A. Rivacoba, M. O. Wolf, and P. M. Echenique, "Cherenkov effect as a probe of photonic nanostructures", *Phys. Rev. Lett.*, Vol. 91, 143902, 2003.
21. Brasch, V., M. Geiselmann, T. Herr, G. Lihachev, M. H. P. Pfeiffer, M. L. Gorodetsky, and T. J. Kippenberg, "Photonic chip-based optical frequency comb using soliton Cherenkov radiation," DOI: 10.1126/science.aad4811, 2015.
22. Schwartz, T., G. Bartal, S. Fishman, and M. Segev, "Transport and Anderson localization in disordered two-dimensional photonic lattices," *Nature*, Vol. 446, 52–55, 2007.
23. Wiersma, D. S., "The physics and applications of random lasers," *Nat. Phys.*, Vol. 4, 359–367, 2008.
24. Burlak, G. and Y. G. Rubo, "Mirrorless lasing from light emitters in percolating clusters," *Phys. Rev. A*, Vol. 92, 013812, 2015.
25. Carusotto, I., M. Artoni, G. C. La Rocca, and F. Bassani, "Slow group velocity and Cherenkov radiation," *Phys. Rev. Lett.*, Vol. 87, 064801, 2001.
26. Udagedara, I., M. Premaratne, I. D. Rukhlenko, H. T. Hattori, and G. P. Agrawal, "Unified perfectly matched layer for finite-difference time-domain modeling of dispersive media," *Opt. Express*, Vol. 7, 22179–21190, 2009.